Frontiers of Information Technology & Electronic Engineering
www.jzus.zju.edu.cn; engineering.cae.cn; www.springerlink.com
ISSN 2095-9184 (print); ISSN 2095-9230 (online)
E-mail: jzus@zju.edu.cn

Motor speed estimation and failure detection of a small UAV using density of maxima*

Jefferson S. SOUZA[1], Moises C. BEZERRIL[1], Mateus A. SILVA[1], Frank C. VERAS[2], Abel LIMA-FILHO[3], Jorge Gabriel RAMOS[4], Alisson V. BRITO[†‡1]

[1]*Laboratory of System Engineering and Robotics, Federal University of Paraiba, Joao Pessoa, Brazil*

[2]*Department of Information Systems, Federal University of Piaui, Picos, Brazil*

[3]*Department of Mechanical Engineering, Federal University of Paraiba, Joao Pessoa, Brazil*

[4]*Department of Physics, Federal University of Paraiba, Joao Pessoa, Brazil*

[†]E-mail: alissonbrito@ci.ufpb.br

Received Apr. 4, 2020; Revision accepted June 9, 2020; Crosschecked Mar. 17, 2021

Abstract: This work presents the application of the technique named signal analysis based on chaos using density of maxima to analyze brushless direct current motors. It uses a correlation coefficient estimated from the density of maxima of the current signal. This study demonstrates in experiments the speed estimation of a brushless motor on a testbench and failure detection in a small flying drone. The experimental results demonstrate that it is possible to estimate the speed in 97.8% of the cases and to detect failure in 82.75% of the analyzed cases.

Key words: Unmanned aerial vehicle (UAV); Speed identification; Failure detection; Chaos
https://doi.org/10.1631/FITEE.2000149 **CLC number:** TP18; V279

1 Introduction

In the past years, there have been advancements in unmanned aerial vehicle (UAV) applications and commercialization (Kuzma et al., 2017; Mills, 2017), in regulation worldwide (Stöcker et al., 2017), and in studies about safety and critical applications, for example, autonomous control technology (Straub and Huber, 2013). Research strives to achieve efficiency and fault tolerance in brushless direct current (BLDC) motors and drones (Lei and Wang, 2019; Nguyen and Hong, 2019; Wang and Wang, 2019; Zhang et al., 2020). Unexpected failures in these motors can be catastrophic, causing financial and human losses.

This work presents the application of the technique named signal analysis based on chaos using density of maxima (SAC-DM) to estimate the speed of a brushless motor and to detect failures in a small drone during flight, by analyzing the vibration signal captured by an accelerometer. The SAC-DM technique estimates the correlation length coefficient (CLC) obtained from the density of maxima. The correlation length reflects the chaotic behavior of the system, and it has been demonstrated by previous work that the technique can estimate the correlation coefficient by the number of peaks in the period signal per time (Bazeia et al., 2017). This approach is computationally simple, and demands a short signal to express the chaotic behavior of the system.

Two contributions are presented in this study: it demonstrates that it is possible to estimate the speed of a BLDC motor on a testbench, calculating just the density of peaks in the vibration signal; furthermore, it is possible to distinguish a healthy

‡ Corresponding author

* Project supported by the Higher Education Improvement Coordination (CAPES) and the National Council for the Scientific and Technological Development (CNPq), Brazil

ORCID: Alisson V. BRITO, https://orcid.org/0000-0001-5215-443X

state from a failure in a more complex scenario with a small flying quadcopter, all performed in the time domain, demanding little computational effort. This allows the applications in real time and for critical scenarios.

The main novelty of the proposed method is its simplicity. The proposed technique is based on counting the number of peaks of the accelerometer signal in the time domain. This means that a simple micro-controller can be used and even a small drone may carry the system without excessive payload. As the approach is based on the chaotic behavior of the system, it is highly sensitive to changes in previous states. The experimental results demonstrate that the accuracy is satisfactory even when a short sample of one second is analyzed.

A new signal processing technique called SAC-DM was devised to estimate the CLC (Medeiros et al., 2018, 2019). These studies demonstrated that it is possible to identify the speed at which the motor is functioning and to detect the presence of an unbalanced propeller by analyzing the motor current signal with SAC-DM. In those cases, one analyzed the current signal collected directly from the BLDC motor. The principle used by SAC-DM comes from nuclear physics, quantum transport in nanostructures, biological systems (Ramos et al., 2011; Bazeia et al., 2017), and cryptography with quantum entanglement (Dietz et al., 2015).

In Veras et al. (2019), SAC-DM was successfully applied to sound signals to detect failures in the same BLDC motor. In the current work, we validate this technique, but to a different signal, using a non-invasive approach that analyzes the mechanical vibration generated by the rotation of the motor on a testbench and the vibration caused by the four engines of a quadcopter during flights, both collect by an accelerometer. Considering the recent worldwide growth in the applications of UAV systems (Kuzma et al., 2017; Mills, 2017; Stöcker et al., 2017), there is demand for research and development of safe and reliable solutions (Yuan et al., 2016; Xiao and Yin, 2017). A game model was applied to design strategies to model the flight characteristics in a multi-UAV scenario (Li et al., 2019).

The motors used in the drone need to receive as much attention as possible. The BLDC motor was used a great deal by industry in machines (Park et al., 2011). Recently, BLDC motors were used as the main alternative for commercial UAV (Solomon, 2007; Tefay et al., 2011; Koteich et al., 2013). The main failures in BLDC motors are stator, rotor, bearing, and inverter faults (Baek et al., 2008). There have been important results in failure detection and safe solutions using these motors. A possible solution is to use model reference adaptive control to improve the speed control of UAV (Solomon, 2007). Another is to use permanent magnet synchronous motors instead of a BLDC motor (Koteich et al., 2013). Also, traditional signal approaches are used a lot, e.g., Fourier transform, motor current signature analysis, wavelets, descriptor observers, and sliding mode observer (Park et al., 2011; Hou et al., 2015; Yang and Yin, 2019a, 2019b; Yang et al., 2020).

2 Signal analysis using chaos based on density of maxima

The density of maxima approach is based on the cyclic equilibrium behavior. In periodic and chaotic systems, the density of peaks (maxima) reflects the chaotic behavior. In the case used here, the chaos is present in the vibration signal generated by a BLDC motor. There have been important contributions in the identification of chaos (Nowak and May, 1992; Mitchell et al., 1993; Károlyi et al., 2005; Gosak et al., 2008). However, previous experiments demonstrated that even in a single and short-time sample, the chaotic behavior can be estimated using the density of maxima (Bazeia et al., 2017; Medeiros et al., 2018, 2019; Veras et al., 2019).

Initially, a quantitative approach that relates the correlation length to the average density of maxima of a signal was presented (Bazeia et al., 2017), where the signal represents the quantity of each biological species along with the simulation. The results proved that the density of maxima can be used to associate the chaotic evolution of the species with the correlation length. Later, the SAC-DM techique was proposed, and it was shown that it can be used to detect failures in BLDC motors using the current signal (Medeiros et al., 2019) and the sound (Veras et al., 2019).

Eq. (1) is applied to analyze samples from non-periodic signals, where $\langle \rho_1 \rangle$ is theoretically calculated by the second and forth derivatives, which are represented as $\mathrm{d}^2C/\mathrm{d}t^2$ and $\mathrm{d}^4C/\mathrm{d}t^4$, respectively, of the auto-correlation function (C) in zero (Bazeia

et al., 2017; Medeiros et al., 2018; Veras et al., 2019):

$$\langle \rho_1 \rangle = \frac{1}{2\pi}\sqrt{-\frac{\frac{\mathrm{d}^4 C}{\mathrm{d}t^4}(0)}{\frac{\mathrm{d}^2 C}{\mathrm{d}t^2}(0)}} = \frac{1}{2\pi}\sqrt{-\frac{\langle q''^2 \rangle}{\langle q'^2 \rangle}}. \quad (1)$$

By the principle of maximum entropy, it is possible to rewrite the normalized correlation function for periodic and homogeneous time series using a cosine function. Thus, Eq. (1) is reduced to

$$\langle \tau \rangle = \frac{1}{6\langle \rho_2 \rangle}, \quad (2)$$

where $\langle \tau \rangle$ is the correlation length and $\langle \rho_2 \rangle$ is the density of maxima found experimentally.

The result found in Eq. (2) presents the chaotic behavior in stochastic systems. It is possible to estimate the characteristics of a system by calculating $\langle \tau \rangle$ for subsets of the signal and analyzing it during the time, or even simply, calculating only $\langle \rho_2 \rangle$. This approach is called SAC-DM, which can be obtained as follows:

$$\text{SAC-DM} = \langle \tau \rangle = \frac{1}{6\langle \rho \rangle}. \quad (3)$$

3 Proving the chaotic behavior

The wavelet discrete transform (WDT) based on the Mallat algorithm (Stéphane , 2009) was applied on signals to extract only the chaotic components. Observing the autocorrelation, the signals collected at the speeds of 70%, 80%, and 90% were processed using the WDT and decomposed into several levels of detail (D). Among the levels of signal decomposition, the detail that presented the chaotic behavior was D5.

The behavior of the wavelet D5 autocorrelation signal applied to the vibration signal of the motor at the speeds of 70%, 80%, and 90% is set out in Fig. 1. After using the filter, it is possible to observe the noise reduction, improving the convergence of the autocorrelation signals.

The CLC (τ_{HH}) can be seen in Fig. 2. It is the value of x for $y = 0.5$ (half-height), which means that the value (τ_{HH}) is 6.759 for the motor at 90% of nominal speed:

$$\tau_{\mathrm{HH}} = X_B - X_A = 7.759 - 1 = 6.759. \quad (4)$$

Fig. 3 presents part of the acceleration signals. From that, it is possible to count 25 697 peaks for

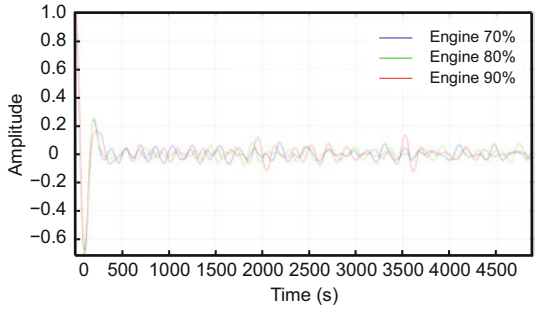

Fig. 1 Autocorrelation curves after filtering by wavelet, with an electronic speed controller at the nominal speeds of 70%, 80%, and 90%

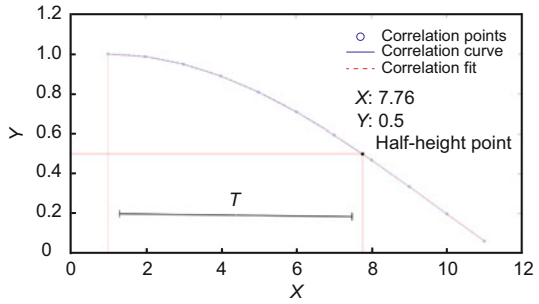

Fig. 2 CLC after filtering by the wavelet function for a motor with the speed at 90% of the motor capacity
The value of τ_{HH} is represented as the value of x for $y = 0.5$, which means CLC=6.759

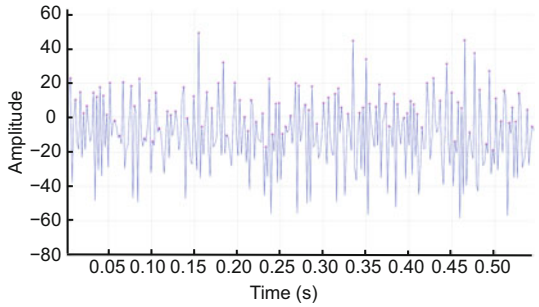

Fig. 3 Example of a vibration signal in zoom with peaks at the speed of 90%, containing 25 697 peaks and SAC-DM=6.4858

a total of 999 999 samples. Calculating the value of SAC-DM from Eq. (3), we have

$$\text{SAC-DM} = \frac{1}{6\frac{25\,697}{999\,999}} = 6.4858. \quad (5)$$

The error found between the CLC obtained from Fig. 2 and the result approximated by SAC-DM in Eq. (5) is 6.485%. When SAC-DM is calculated for all signals, the error decreases to 4.0542%. These results are shown in Table 1.

Considering that the values of the errors in all measurements are less than 7%, it can be stated that the vibration signal analyzed and discussed here has

a chaotic behavior and can be driven by calculations involving Eq. (3).

4 Methodology

The approach applied to this work is divided into four steps. First, an accelerometer connected to a 32-bit RISC-V microcontroller unit (MCU) collects the vibration signal. Then, the vector sum $\boldsymbol{x} + \boldsymbol{y}$ is calculated. Thereafter, the result is used to calculate SAC-DM from Eq. (5). Finally, from the values of SAC-DM, one can estimate the speed of the BLDC motor and detect failures in a small UAV.

4.1 Accelerometer signal acquisition

A testbench was built to collect data and validate the results. Fig. 4 shows the experimental setup of the BLDC motor. Table 2 presents the specifications of the testbench.

The testbench consists of the following: (1) a BLDC motor of 1400 kV; (2) an accelerometer Adafruit ADXL345; (3) a node MCU ESP 8266 12F Arduino based microcontroller, to set the speed sent to the electronic speed controller (ESC); (4) an ESC of 30 A; (5) a 10.4-inch propeller.

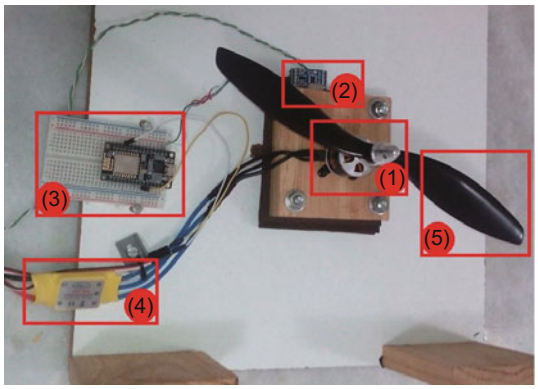

Fig. 4 Testbench to collect vibration generated by the BLDC motor
(a) BLDC motor; (b) accelerometer; (c) microcontroller; (d) ESC; (e) 10.4-inch propeller

Table 1 Values for CLC collected from the autocorrelation function, i.e., SAC-DM in Eq. (3), and the respective error

Speed (%)	CLC	SAC-DM	Error (%)
70	6.7215	6.4526	3.9992
80	6.8880	6.4634	6.1636
90	6.4858	6.7599	4.0542

Table 2 BLDC motor specifications

Description	Value	Unit	Description	Value	Unit
DC voltage	12	V	Weight	59	g
Rated speed	930	r/min	Power	270	W

4.2 SAC-DM

With the sum of the acceleration vectors, $\boldsymbol{x}+\boldsymbol{y}$, the density of maxima of a predefined group of samples was calculated. Eq. (5) was applied and SAC-DM was obtained. SAC-DM was calculated according to Eq. (3) for each subset of the time series collected by the accelerometer. After calculation for each subset, it was checked whether the value of SAC-DM was within the expected range for a balanced motor. If not, it returned that it is unbalanced. From the calculated SAC-DM, the estimated motor speed was returned.

5 Speed detection

After data collection, five experimental scenarios were defined to evaluate the system, with different numbers of samples per time for the calculation of SAC-DM, and each executed with three different speeds (70%, 80%, and 90%):

group 1: SAC-DM calculated for each 200 samples; group 2: SAC-DM calculated for each 400 samples; group 3: SAC-DM calculated for each 600 samples; group 4: SAC-DM calculated for each 800 samples; group 5: SAC-DM calculated for each 1000 samples.

From the tests, a total of one million and eight hundred thousand samples were collected for each speed (70%, 80%, and 90%), with a sampling frequency of 520 Hz, totaling five million and four hundred thousand samples.

Using the accelerometer ADXL345 from Adafruit, it is possible to collect data under three actuation axes (X, Y, and Z). Considering that the Z axis was directed to the depth dimension of the bench, it was ignored for SAC-DM calculations. Thus, the sum of the vectors, $\boldsymbol{x} + \boldsymbol{y}$, was used to calculate SAC-DM.

Other essential conditions for the experimental scenario are acquisition rates and accelerometer calibrations. The accelerometer worked in the range of 1 to 3.2 kHz, and the responsiveness from 2G to 16G for the experiment was used with an acquisition rate of 1.6 kHz and sensitivity of 16G (here, G means the gravity force).

In the experiment, SAC-DM was calculated for every 1000 samples of the acceleration vector. It is possible to identify an accuracy greater than 97% in all scenarios.

In Fig. 5, the values of SAC-DM for each group of 1000 samples are shown for speeds of 70%, 80%, and 90%. It is possible to see the distribution of SAC-DM values and the intersection between them. These approximations and overlaps are ranges where the speed estimate is less accurate.

Fig. 6 shows the distribution of the SAC-DM values for every 1000 samples. The intersection area between the histograms relate to cases where speed estimate would be less accurate. Such regions correspond to 0.3% between the speeds of 70% and 80% and 4.1% between the speeds of 80% and 90%, which means 97.8% of accuracy on average.

6 Fault detection

An experiment was assembled to collect the values of SAC-DM calculated from the vibration via the accelerometer, and to submit all the data to a database service to allow real-time visualization and future analysis (Fig. 7). The experiment was divided into two parts, the cloud service and the hardware embedded on the drone.

On the drone side, an ESP8266 micro-controller with an accelerometer was embedded to capture the vibration and calculate the SAC-DM value. It sent all the data instantly to the cloud service through a WiFi connection. On the cloud service side, there was a back-end hosted in the firebase service that received the SAC-DM values, stored and then sent them to the client-side interface, which built a visualization in real time. The specification of components used in the experiment is presented in Table 3.

The experiments consist of five flights of 5 min each, controlled by the same person who tried to perform the same movements (only smooth movements). Among the five flights, three were presented with two types of drone failures, one with the combination of two defeats, and one with the drone in the stable state, without problems.

For the first flight, all the drone propellers were balanced, and the battery was in the central position to keep the center of gravity in the right place, representing the drone in the stable state.

The first failure added to the drone was with a 10 cm piece of tape glued on the top of the frontal right propeller, generating a propeller unbalance

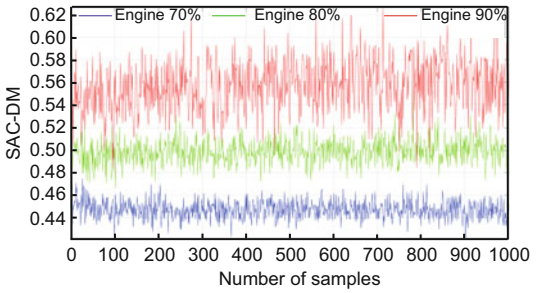

Fig. 5 SAC-DM values for acceleration with nominal speeds of 70%, 80%, and 90% of a motor

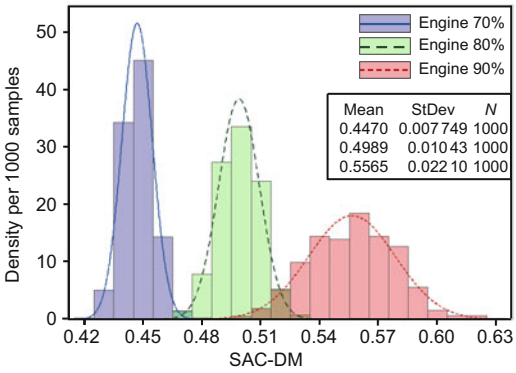

Fig. 6 Histogram of SAC-DM calculated from the acceleration vector signal for 70%, 80%, and 90% speeds

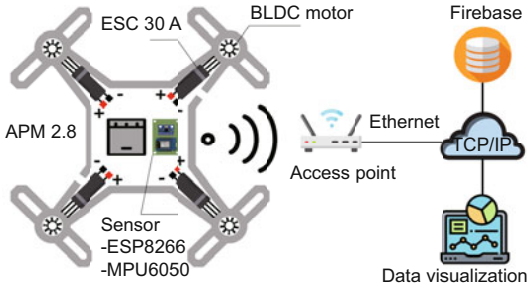

Fig. 7 Architecture to collect data from the UAV, with an access point to connect the Internet via TCP/IP, a database (firebase), and a web interface for real-time visualization

Table 3 Small UAV specifications

Parameter	Value
Frame size (cm×cm)	46×46
Motor voltage (kV)	920
Propeller size	10
Propeller pitch	45
Weight (kg)	1.02
Max thrust (kg)	3.44 (860 g per motor)
Battery	3 cells with 2800 mA·h
Flight controller	APM 2.8

APM: Ardupilot module

failure. The second failure was changing the center of gravity. For this, the battery was moved 7.5 cm from the drone center. For the third unstable condition, the tape was applied on the propeller and the battery position for both failures.

For all tests, a threshold in the amplitude of 10% was adopted to calculate the density of maxima (SAC-DM). It means that a hill in the signal will be counted as a peak only if the top is 10% higher than its basis. This approach reduced the error caused by noise. The values from the accelerometer were captured at 500 Hz, and at each second, 500 values are used to compute one SAC-DM value. It was observed that the results obtained from SAC-DM calculated from vibration in the X and Z axes were accurate in detecting failures related to unbalanced propellers, even analyzing over only 1 s.

The dispersion of the SAC-DM values for the X and Z axes is presented in Figs. 8 and 9, respectively. In both cases, the gravity center (GC) was correctly in the center of the drone, but one of the propellers was unbalanced, first with one tape, and then with two tapes. Observing the X axis shown in Fig. 8, we can see that, it is possible to differentiate an imbalance in a propeller with SAC-DM. There was a visible difference between the stable scenario and the unbalanced propeller scenarios. This difference was even more evident when we analyzed the results from the Z axis (Fig. 9). When the drone was stable, values of SAC-DM were between 0.21 and 0.31, while those for the unbalanced propeller with one tape were between 0.18 and 0.25, and those with two tapes were between 0.12 and 0.20.

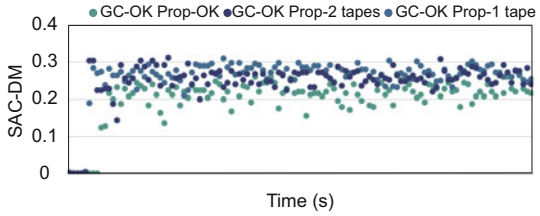

Fig. 8 Dispersion of SAC-DM values for vibrations in the X axis when the propeller has one or two tapes (threshold=10% and rate=500 Hz)

Three scenarios are presented, with the regular propeller and the unbalanced propeller with one or two tapes

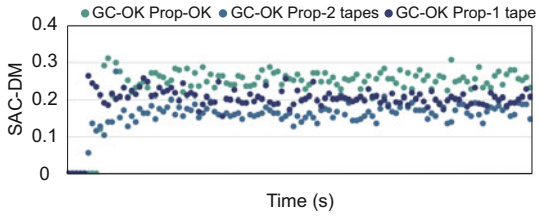

Fig. 9 Dispersion of SAC-DM values for vibrations in the Z axis when the propeller has one or two tapes (threshold=10% and rate=500 Hz)

The gravity center (GC) is not changed. Three scenarios are presented, with the regular propeller and the unbalanced propeller with one or two tapes

A similar result was achieved when the GC was changed in Fig. 10. Here, there was an even more apparent difference between the balanced and unbalanced propeller scenarios. In Fig. 11, the values of SAC-DM in the Z axis for the situation with a balanced propeller were in a range separated (between 0.2 and 0.3) from the unbalanced cases (between 0.15 and 0.20). Nevertheless, the values for one and two tapes presented a higher intersection.

These results are summarized in Table 4. It presents the success rate when SAC-DM was used as a reference to detect failures in the small UAV. The approach applied here to classify each value was based on the range of average SAC-DM, more or less the standard deviation. Only two classes were defined, a failure or not a failure. For each analysis, only one value of SAC-DM was used for classification.

For example, once the GC was correctly set,

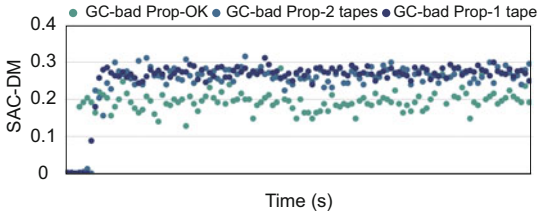

Fig. 10 Dispersion of SAC-DM values for vibrations in the X axis when GC is not centralized (bad GC, threshold=10%, and rate=500 Hz)

Three scenarios are presented with GC modified, with the regular propeller and the unbalanced propeller with one or two tapes

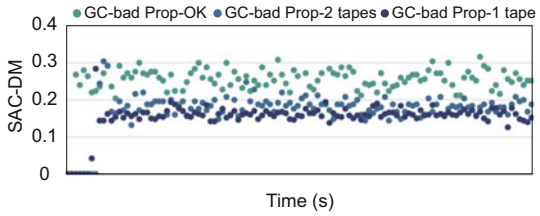

Fig. 11 Dispersion of SAC-DM values for vibrations in the Z axis when GC is not centralized (bad GC, threshold=10%, and rate=500 Hz)

Three scenarios are presented with GC modified, with the regular propeller and the unbalanced propeller with one or two tapes

for 99.1% of the SAC-DM values, the classifier successfully detected the failure in the UAV when two tapes were glued on the propeller, and classified the failure correctly in 87.6% of cases with one tape. On average, when the GC was correct, the classification was successful in 88.37% of the cases. The same analysis was presented when the GC was not the center of the UAV. The detection when the propeller was balanced was successful only in 33.1% of the cases, returning, however, the correct classification in 100% and 98.3% of the cases with one and two tapes on the propeller, respectively. In general, the success rate of detection was 82.75%. It means that in 82.75% of the cases, only SAC-DM=1 is enough to identify whether the UAV has a failure or not.

Table 4 Accuracy in the failure detection considering SAC-DM from the *Z* axis, grouped by change in the propeller and in the gravitation center

Propeller	Accuracy		Average
	GC-OK	GC-bad	
OK	78.4%	33.1%	**55.75%**
One tape	87.6%	100%	**93.80%**
Two tapes	99.1%	98.3%	**98.70%**
Average	**88.37%**	**77.13%**	**82.75%**

The results in bold represent the average accuracy for each line and column

7 Conclusions

When analyzing the BLDC motor isolated, the average of SAC-DM is 0.4470 for the speed at 70% of the maximum power, 0.4989 for 80%, and 0.5565 for 90%. Although the percentages were different, it is possible to see that there was a short range of values where SAC-DM was the same for 80% and 90%. This result proves the possibility of applying the presented technique to estimate the speed of a motor using a computationally simple approach, counting only the density of peaks in the time domain, without any filtering.

Accuracies of 82.75% on average and 100% in the best case were achieved for the tests with a small UAV, which demonstrates the efficiency of the proposed method. The algorithm used to detect failure is based only on testing whether a value is in a fixed range or not. Five hundred samples of acceleration in the time domain were used to calculate each value of SAC-DM at each second. In other words, only one second is enough to achieve the accuracy of 82.75%, and it could be increased if more extended analysis with more values was used. A limitation of the method is its difficulty in failure diagnosis. Due to its sensibility, even weak disturbances in the system can be detected. This might reduce the accuracy in failure diagnosis. Nevertheless, the accuracy is high to simply detect whether there is a failure or not. In future work, we plan to apply SAC-DM integrated with artificial neural networks to minimize this limitation.

Contributors

Jefferson S. SOUZA and Frank C. VERAS designed the research. Jefferson S. SOUZA, Moises C. BEZERRIL, and Matheus A. SILVA performed the experiments and processed the data. Alisson V. BRITO drafted the manuscript. Abel LIMA-FILHO and Jorge Gabriel RAMOS helped organize the manuscript and the math formalism. Alisson V. BRITO revised and finalized the paper.

Compliance with ethics guidelines

Jefferson S. SOUZA, Moises C. BEZERRIL, Mateus A. SILVA, Frank C. VERAS, Abel LIMA-FILHO, Jorge Gabriel RAMOS, and Alisson V. BRITO declare that they have no conflict of interest.

References

Baek G, Kim Y, Kim S, 2008. Fault diagnosis of identical brushless DC motors under patterns of state change. Proc IEEE Int Conf on Fuzzy Systems (IEEE World Congress on Computational Intelligence), p.2083-2088. https://doi.org/10.1109/FUZZY.2008.4630657

Bazeia D, Pereira MBPN, Brito AV, et al., 2017. A novel procedure for the identification of chaos in complex biological systems. *Sci Rep*, 7:44900.

Dietz B, Richter A, Samajdar R, 2015. Cross-section fluctuations in open microwave billiards and quantum graphs: the counting-of-maxima method revisited. *Phys Rev E*, 92(2):022904.

Gosak M, Marhl M, Perc M, 2008. Chaos between stochasticity and periodicity in the prisoner's dilemma game. *Int J Bifurc Chaos*, 18(3):869-875.

Hou WQ, Zhang YX, Sun JP, 2015. A fault detection method for motors based on local polynomial Fourier transform. Prognostics and System Health Management Conf, p.1-5. https://doi.org/10.1109/PHM.2015.7380056

Károlyi G, Neufeld Z, Scheuring I, 2005. Rock-scissors-paper game in a chaotic flow: the effect of dispersion on the cyclic competition of microorganisms. *J Theory Biol*, 236(1):12-20.

Koteich M, Le Moing T, Janot A, et al., 2013. A real-time observer for UAV's brushless motors. IEEE 11th Int Workshop of Electronics, Control, Measurement, Signals and Their Application to Mechatronics, p.1-5. https://doi.org/10.1109/ECMSM.2013.6648964

Kuzma J, O'Sullivan S, Philippe T, et al., 2017. Commercialization strategy in managing online presence in the unamanned aerial vehicle industry. *Int J Bus Strat*, 17(1):59-68. https://doi.org/10.18374/IJBS-17-1.6

Lei Y, Wang JL, 2019. Aerodynamic performance of quadrotor UAV with non-planar rotors. *Appl Sci*, 9(14):2779. https://doi.org/10.3390/app9142779

Li YM, Du WB, Yang P, et al., 2019. A satisficing conflict resolution approach for multiple UAVs. *IEEE Intern Things J*, 6(2):1866-1878.

Medeiros RLV, Ramos JGGS, Nascimento TP, et al., 2018. A novel approach for brushless DC motors characterization in drones based on chaos. *Drones*, 2(2):14. https://doi.org/10.3390/drones2020014

Medeiros RLV, Filho ACL, Ramos JGGS, et al., 2019. A novel approach for speed and failure detection in brushless DC motors based on chaos. *IEEE Trans Ind Electron*, 66(11):8751-8759. https://doi.org/10.1109/TIE.2018.2886766

Mills MP, 2017. Drone disruption: the stakes, the players, and the opportunities. https://www.forbes.com/sites/markpmills/2016/03/23/drone-disruption-the-stakes-the-players-and-the-opportunities/#58333ffe7d0b

Mitchell M, Hraber P, Crutchfield JP, 1993. Revisiting the edge of chaos: evolving cellular automata to perform computations. https://arxiv.org/abs/adap-org/9303003

Nguyen NP, Hong SK, 2019. Active fault-tolerant control of a quadcopter against time-varying actuator faults and saturations using sliding mode backstepping approach. *Appl Sci*, 9(19):4010. https://doi.org/10.3390/app9194010

Nowak MA, May RM, 1992. Evolutionary games and spatial chaos. *Nature*, 359(6398):826-829. https://doi.org/10.1038/359826a0

Park BG, Lee KJ, Kim RY, et al., 2011. Simple fault diagnosis based on operating characteristic of brushless direct-current motor drives. *IEEE Trans Ind Electron*, 58(5):1586-1593. https://doi.org/10.1109/TIE.2010.2072895

Ramos JGGS, Bazeia D, Hussein MS, et al., 2011. Conductance peaks in open quantum dots. *Phys Rev Lett*, 107(17):176807. https://doi.org/10.1103/PhysRevLett.107.176807

Solomon O, 2007. Model reference adaptive control of a permanent magnet brushless DC motor for UAV electric propulsion system. Proc 33rd Annual Conf of the IEEE Industrial Electronics Society, p.1186-1191. https://doi.org/10.1109/IECON.2007.4460304

Stéphane M, 2009. A Wavelet Tour of Signal Processing (3rd Ed.). Academic Press, Amsterdam, Boston, USA. https://doi.org/10.1016/B978-0-12-374370-1.X0001-8

Stöcker C, Bennett R, Nex F, et al., 2017. Review of the current state of UAV regulations. *Remot Sens*, 9(5):459. https://doi.org/10.3390/rs9050459

Straub J, Huber J, 2013. Validating a UAV artificial intelligence control system using an autonomous test case generator. Airborne Intelligence, Surveillance, Reconnaissance Systems and Applications X, Article 87130I. https://doi.org/10.1117/12.2018591

Tefay B, Eizad B, Crosthwaite P, et al., 2011. Design of an integrated electronic speed controller for compact robotic vehicles. Proc Australasian Conf on Robotics and Automation, p.2083-2088.

Veras FC, Lima TLV, Souza JS, et al., 2019. Eccentricity failure detection of brushless DC motors from sound signals based on density of maxima. *IEEE Access*, 7:150318-150326. https://doi.org/10.1109/ACCESS.2019.2946502

Wang W, Wang JW, 2019. Dynamic response enhancement and fault protection of boost converter-fed brushless DC motor in aerospace applications. *Appl Sci*, 9(10):2113. https://doi.org/10.3390/app9102113

Xiao B, Yin S, 2017. A new disturbance attenuation control scheme for quadrotor unmanned aerial vehicles. *IEEE Trans Ind Inform*, 13(6):2922-2932. https://doi.org/10.1109/TII.2017.2682900

Yang HY, Yin S, 2019a. Descriptor observers design for Markov jump systems with simultaneous sensor and actuator faults. *IEEE Trans Autom Contr*, 64(8):3370-3377. https://doi.org/10.1109/TAC.2018.2879765

Yang HY, Yin S, 2019b. Reduced-order sliding-mode-observer-based fault estimation for Markov jump systems. *IEEE Trans Autom Contr*, 64(11):4733-4740. https://doi.org/10.1109/TAC.2019.2904435

Yang HY, Jiang YC, Yin S, 2020. Adaptive fuzzy fault tolerant control for Markov jump systems with additive and multiplicative actuator faults. *IEEE Trans Fuzzy Syst*, online. https://doi.org/10.1109/TFUZZ.2020.2965884

Yuan Y, Yuan HH, Guo L, et al., 2016. Resilient control of networked control system under DoS attacks: a unified game approach. *IEEE Trans Ind Inform*, 12(5):1786-1794. https://doi.org/10.1109/TII.2016.2542208

Zhang Q, Chen X, Xu DZ, 2020. Adaptive neural fault-tolerant control for the yaw control of UAV helicopters with input saturation and full-state constraints. *Appl Sci*, 10(4):1404. https://doi.org/10.3390/app10041404